Hydrothermal crystal growth of the potassium niobate and potassium tantalate family of crystals

Matthew Mann [a,b], Summer Jackson [a], Joseph Kolis [a,b],*

[a] Department of Chemistry, Clemson University, Clemson, SC 29634, USA
[b] Center for Optical Materials Science and Engineering Technologies (COMSET), 91 Technology Drive, Anderson, SC 29625, USA

A B S T R A C T

Single crystals of $KNbO_3$ (KN), $KTaO_3$ (KT), and $KTa_{1-x}Nb_xO_3$ ($x=0.44$, KTN) have been prepared by hydrothermal synthesis in highly concentrated KOH mineralizer solutions. The traditional problems of inhomogeneity, non-stoichiometry, crystal striations and crystal cracking resulting from phase transitions associated with this family compounds are minimized by the hydrothermal crystal growth technique. Crystals of good optical quality with only minor amounts of metal ion reduction can be grown this way. Reactions were also designed to provide homogeneous distribution of tantalum and niobium metal centers throughout the KTN crystal lattice to maximize its electro-optic properties. Synthesis was performed at relatively low (500–660 °C) temperatures in comparison to the flux and Czochralski techniques. This work represents the largest crystals of this family of compounds grown by hydrothermal methods to date.

1. Introduction

The synthesis and crystal growth of the $KTaO_3$-$KTa_{1-x}Nb_xO_3$-$KNbO_3$ (KT–KTN–KN) family is of interest due to the attractive properties and potential applications for each member. For instance, $KNbO_3$ has desirable nonlinear optical properties useful for generating blue laser light while at the other stoichiometric limit, $KTaO_3$ is a photocatalyst used in the decomposition of H_2O [1]. KTN, the solid solution phase of these two materials has very desirable photorefractive and electro-optic properties useful for waveguide applications. These applications have very different dimensional requirements. NLO applications would ideally require $KNbO_3$ crystals in excess of 1 cm^3, while use of $KTaO_3$ as a photocatalyst would need uniform nano to micron sized particles. With the differing applications and size requirements, there has not been an encompassing study of this system by any one crystal growth technique. A correction of this unfortunate oversight could lead to greater understanding of this series of compounds.

Of this family of compounds the Amm_2 acentric orthorhombic phase of potassium niobate (KN) has been the most extensively studied member. Over the past 35 years measurements have identified outstanding piezoelectric, electro-optical, nonlinear optical, and photorefractive properties of Amm_2 KN [2–8]. With such diverse qualities, applications for the orthorhombic phase include second harmonic generation of blue lasers [9,10], holographic storage [8,11], and surface acoustic wave (SAW) devices [12]. Despite numerous attempts to synthesize high quality crystals using classical high temperature techniques, such as flux [13–15], top seeded solution growth (TSSG) [12,16–18], Kyropoulus [19–21], floating zone technique [22,23], and vertical Bridgman technique, crystal quality has been hampered by non-stoichiometry, inhomogeneity, metal reduction, striations, and most importantly, crystal cracking.

Similar to KN, inhomogeneous growth is a major difficulty associated with KTN synthesis. To acquire the optimum ferroelectric performance, the ratio of tantalum to niobium must be controlled and evenly distributed throughout the crystal. The properties and the crystallographic phase of KTN depend greatly on both of these requirements. Most desirable is the cubic form of KTN with a Curie temperature slightly above room temperature. A composition of $KTa_{0.60}Nb_{0.40}O_3$ would optimize the large electro-optic coefficient with a Curie temperature near 35 °C [24]. Unfortunately, homogeneous crystallization of this ratio has proven difficult for many crystal growth techniques. KTN growth by melt [25], Czochralski [26], and TSSG [27–29] has also been frustrated by striation problems similar to those encountered with KN growth. Other methods such as flux growth have dealt with solvent inclusions, repeatability, and flux volatilization [30]. Some preliminary success however was established in hydrothermal fluids by Marshall and Laudise [31], who demonstrated growth to a seed with a positive solubility relationship with temperature.

In contrast to KN and KTN, growth of large $KTaO_3$ (KT) crystals has not received much interest. Rather, powders and thin films

* Corresponding author at: Department of Chemistry, Hunter Labs, Clemson University, Clemson, SC 29634-0973, USA. Fax: +1 864 656 6613.
E-mail address: kjoseph@clemson.edu (J. Kolis).

have garnered the most attention in regards to growth of KT. It is considered to be one of the best materials for photocatalytic decomposition of H_2O into H_2 and O_2 [32]. For such applications, particle size must be constricted to nanometer to micron sized single crystals. These small particles are typically synthesized by epitaxial [33], chemical solution deposition [34,35], polymeric precursor method [36], solvothermal [37], and hydrothermal methods [38]. Growth conditions for large single crystals have not been studied due to a lack of real applications. Nevertheless, an understanding of the phase relationship and a good synthesis route to KT crystals would be of interest.

The practical crystal growth difficulties that must be overcome for these materials are not trivial. Hydrothermal synthesis has been capable of addressing many of these concerns in other materials. Yet this growth technique has only been briefly investigated for this family of compounds. Studies have been limited to nano-sized particles in most cases. Thus far the bulk of hydrothermal work performed on KN has occurred at subcritical temperatures in Teflon lined Parr bombs. One of only two supercritical studies, Li used low concentrations of potassium hydroxide to generate micron size KN crystals over the course of 24 h [3]. While still many orders of magnitude too small for practical applications, it demonstrates an increase over the nano-sized particles found in subcritical reactions. The most surprising discovery was the direct crystallization of the orthorhombic phase, despite being above the KN phase transition temperature.

Growth of the orthorhombic phase is quite common in subcritical hydrothermal reactions, but is unexpected in supercritical reactions since it is above the phase transition. At these temperatures, crystallization of the tetragonal phase should be preferential, yet this is not the case. It is unknown as to why the orthorhombic phase is stabilized in hydrothermal fluids above its transition point. This is a fortuitous result however, since the formation of the *Amm2* phase directly during the growth process will prevent the realignment cracking associated with the phase change during cooling, as happens with other high temperature growth methods. This considerable advantage coupled with the ability of hydrothermal solutions to control homogeneity and limit striations is attractive, which merits further research and exploitation. Thus a hydrothermal investigation was undertaken to study solubility, homogeneity, and metal reduction inside the $KTaO_3 - KTa_{1-x}Nb_xO_3$-$KNbO_3$ family.

2. Experimental

2.1. Hydrothermal synthesis

Single crystals of $KNbO_3$, $KTaO_3$, and $KTa_{1-x}Nb_xO_3$ were prepared by hydrothermal synthesis. For spontaneous nucleation reactions a feedstock of the desired material was loaded into silver ampoules (Stern Leach, 99.99%) with varying dimensions of $1/4$–$3/8''$ inner diameter and lengths of 2.5–8″. After a mineralizer solution of either KOH (MV Laboratories, 99.99%) or KF (Alfa Aesar, 99.9%) was added, the ampoule was welded shut and then placed into a 27 mL internal volume Inconel autoclave. The remaining volume of the autoclave was filled with deionized water to serve as counter pressure to prevent the ampoules from bursting. The autoclave was then heated to temperatures ranging from 400 to 660 °C for 5–20 days resulting in pressures of 10,000–25,000 psi. When the reaction was deemed complete the silver ampoules were retrieved from the autoclave and then opened with the contents being flushed onto filter paper using deionized water. The resultant products were characterized by single crystal X-ray diffraction and energy dispersive X-ray analysis.

2.2. Solid state synthesis

All spontaneous nucleation and bulk growth reactions were performed with an initial feedstock of the desired material. A feedstock of $KNbO_3$ (Alfa Aesar, 99.999%) was commercially available, however powders of $KTaO_3$ and $KTa_{1-x}Nb_xO_3$ had to be prepared by solid state reactions. A stoichiometric ratio of K_2CO_3 (Alfa Aesar, 99.997%) and Ta_2O_5 (Alfa Aesar, 99%) powders were ground and heated to 950 °C for 72 h and confirmed as $KTaO_3$ by powder X-ray diffraction. A KTN feedstock of a specific composition could be prepared by a similar method, although after powders of K_2CO_3, Ta_2O_5, and Nb_2O_5 (Strem, 99.9%) were mixed a pellet was form using 10,000 psi of pressure. This minimizes small grains of KN or KT that form when heating a loose powder. The pellet was heated to 950 °C for 24 h and then ground and repressed followed by subsequent heating for an additional 24 h period. This procedure was repeated for 72 h and then confirmed as $KTa_{1-x}Nb_xO_3$, where $x = 0.40$, by powder X-ray diffraction.

2.3. Characterization

2.3.1. X-ray powder and single crystal diffraction

Powder X-ray analysis on the feedstock of KT and KTN were performed on a Scintag XDS 2000 diffractometer using Cu$K\alpha$ ($\lambda = 1.54056$ Å). All samples were collected in the step scan mode with a 0.03° step size over a 2θ range of 5–65°. Single crystal X-ray analysis was performed on a Rigaku AFC8 diffractometer equipped with a Mercury CCD area detector and a sealed graphite monochromated tube used to generate Mo$K\alpha$ ($\lambda = 0.71073$ Å) radiation. The crystal structures were solved by direct methods using Shelxtl-97 and refined using least-squares techniques [39].

2.3.2. Energy dispersive X-ray analysis

Elemental analysis and elemental mapping was performed using a simultaneous Hitachi S-3400N scanning electron microscopy equipped with an Oxford INCA energy dispersive X-ray analysis detector. Several data points were collected on samples in an evacuated chamber with an accelerating 20 kV electron beam.

2.3.3. Infrared analysis

Infrared analysis was performed on ground crystalline samples of KT, KTN, and KN using a Nicolet Magma 550 IR spectrometer. The powder was incorporated into a KBr matrix that was used to form a transparent pellet, which was examined from 4000 to 400 cm^{-1}.

3. Results and discussion

3.1. Spontaneous nucleation of $KNbO_3$

Hydrothermal research to this point has used Nb_2O_5 and excess KOH as starting reagents to produce $KNbO_3$. Formation of potassium niobate by this method consumes a portion of the potassium hydroxide mineralizer [40,41]. This manner of synthesis is very undesirable because the conditions inside the vessel are constantly changing over time. Thus it becomes very difficult to assess the true validity of the mineralizer as a crystal growth medium. Therefore to ensure a consistent environment, all reactions were performed with a feedstock of $KNbO_3$ powder. Beyond guaranteeing a stable mineralizer concentration, starting with a feedstock of the desired target material generally ensures better size and quality of the resultant crystals.

Previous hydrothermal studies showed that potassium hydroxide mineralizers are capable of crystallizing the orthorhombic KN phase at both sub and supercritical temperatures [3,41]. Regardless of the desired phase, the overall sizes of the crystals were quite limited. Therefore other mineralizer solutions were briefly explored by us. The only successful growth of $KNbO_3$ was found in potassium fluoride. Growth in this medium lead to the orthorhombic phase of KN, but the crystals had a fibrous morphology (Fig. 1a). Continued growth under these conditions would be unsuitable for bulk transport growth based on the dimensionality of these crystals, therefore KOH mineralizers were used exclusively from this point.

Reactions performed in solutions of 6 M KOH at 400 °C resulted in a crystalline powder which was determined to be the orthorhombic *Amm2* $KNbO_3$ phase by powder X-ray diffraction. While the direct synthesis of the acentric phase is encouraging, there is little improvement over Li's work when considering the size of the crystals [3]. To increase the dimensions, greater solubility of $KNbO_3$ was required. Thus the reaction temperature was raised from 400 to 575 °C while maintaining the 6 M mineralizer concentration for the same time period. The resultant crystals, Fig. 1b, were considerably larger at 0.5 mm per edge and were slightly opaque. The desirable orthorhombic phase is still maintained despite synthesis at higher temperatures. To date these are the largest hydrothermal grown crystals of $KNbO_3$, yet these crystals are too small for use as seeds in transport reactions (approximately 3 mm). However, no spontaneous crystals thus far have exceeded this size and continued work in this temperature regime, with only slight changes in the mineralizer, did not yield crystals with greater dimensions.

An increase in temperature from 400 to 575 °C was accompanied by approximately a 10 fold increase in size of spontaneous KN crystals. Thus, the temperature for large crystal growth was subsequently increased to 640 °C, while also using an extremely concentrated solution of potassium hydroxide. In Fig. 1c, crystals several millimeters long were spontaneously grown from a 14 M KOH solution. While dimensions were improved, the crystals exhibited striations and discoloration. The resultant blue color can be attributed to oxygen dislocations, which are compensated for by a reduction of the niobium metal center.

There was some concern that the striations were from the initial formation of either the tetragonal or cubic KN phase, followed by cooling through these phase transitions. To improve quality, the growth rate was slowed significantly by decreasing the temperature to 490 °C, while retaining the previous 14 M KOH concentration. The resultant crystals, Fig. 1d, were of excellent quality with both the striations and coloration removed.

A single crystal structure of the orthorhombic KN from this reaction was solved down an *R*-factor of 0.0215. The remaining crystallographic data is presented in Table 1. If the crystal had undergone any phase transitions, it is unlikely that such high quality diffraction data could have been obtained, which suggest the direct formation of the desirable *Amm2* phase above its transition temperature. Growth in solution at a pressure of 17,000 psi may play some role in stabilizing this phase, but the exact reason is not known. Despite incomplete comprehension of the crystallization process, growth of high quality orthorhombic KN crystals has been achieved using hydrothermal methods.

3.2. Spontaneous nucleation of $KTaO_3$

The primary goal of our work is growth of large KT crystals to understand the behavior of tantalates in hydrothermal fluids. This knowledge will prove useful when growing KTN with varying degrees of tantalum and niobium ratios. Only micron sized particles of cubic KT have been synthesized previously. Hydrothermal production of these small particles has been established in KOH mineralizers at relatively low temperatures and pressures [38]. Like $KNbO_3$, hydrothermal reactions in the supercritical regions have not been extensively explored.
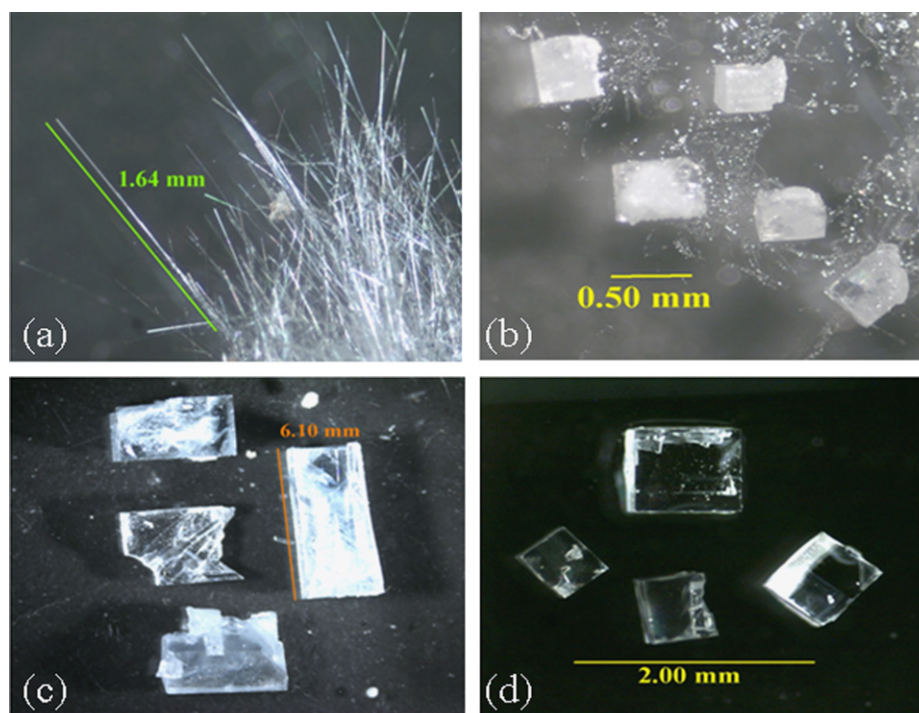

Fig. 1. (a) Fibrous growth of orthorhombic KN in potassium fluoride solutions; (b) orthorhombic KN crystals grown at 575 °C in potassium hydroxide; (c) large growth of orthorhombic KN crystals at 640 °C; (d) high quality growth of orthorhombic KN crystals at 490 °C.

Table 1
Crystallographic data for KT–KTN–KN.

Chemical formula	KNbO$_3$	KTaO$_3$	KTa$_{1-x}$Nb$_x$O$_3$ (x=0.45)
F. W. (g/mol)	180.01	268.05	232.83
Space group	$Amm2$ (No. 38)	Pm-$3m$ (No. 221)	Pm-$3m$ (No. 221)
Crystal system	Orthorhombic	Cubic	Cubic
a, Å	3.9746(8)	3.9895(5)	3.9978(5)
b, Å	5.6948(11)		
c, Å	5.7148(11)		
V, Å	129.35(4)	63.497(14)	63.894(14)
Z	2	1	1
D_{cal}, mg/m	4.622	7.010	5.937
Indices (min)	[−5,−7,−7]	[−4,−4,−5]	[−5,−5,−6]
(max)	[4,6,6]	[5,5,5,]	[5,5,4]
Parameters	20	6	7
Restraints	1	0	0
μ, mm	5.995	44.644	27.132
2θ range, deg.	5.05–27.11	5.11–27.01	5.10–32.73
Reflections			
Collected	515	567	609
Unique	157	28	40
R(int)	0.0458	0.0590	0.0438
Final R (obs. data)[a]			
R_1	0.0215	0.0131	0.0109
wR_2	0.0472	0.0302	0.0249
Final R (all data)			
R_1	0.0221	0.0187	0.0109
wR_2	0.0472	0.0314	0.0249
Extinction coeff.	1.02(12)	0.27(4)	1.7(3)
Goodness of fit (S)	1.115	1.149	1.207
Flack parameter	−0.2(4)	N/A	N/A
Largest diff. Peak, e/Å	0.825	0.980	0.756
Largest diff. Hole, e/Å	−0.904	−0.866	−0.668

[a] $R_1 = [\Sigma ||F_0| - |F_c||]/\Sigma |F_0|$; w$R_2 = \{[\Sigma w[(F_0)^2 - (F_c)^2]^2]\}^{1/2}$.
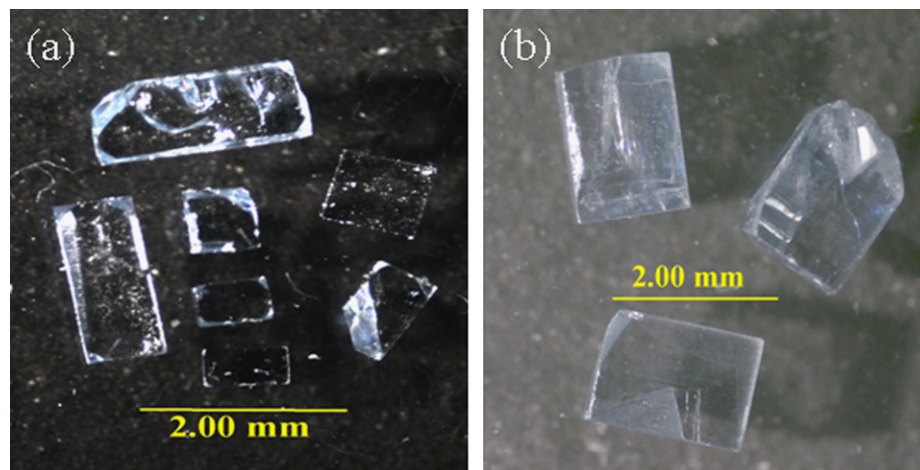

Fig. 2. (a) KTaO$_3$ crystals grown in hydrothermal solutions of 30 M KOH at 640 °C; (b) Slightly reduced KTN crystals grown in hydrothermal solutions of 30 M KOH at 660 °C.

The most obvious starting point for growth of KT crystals is the same conditions which provided KN. A feedstock of KTaO$_3$ powder was used in a hydrothermal reaction performed at 490 °C in 14 M KOH. Unfortunately these conditions did not provide crystal growth comparable to the KNbO$_3$ results. Instead only micro-crystalline powder of cubic KT was produced under these conditions. When the synthesis temperature was raised to 600 °C this also had little effect, with KT crystal dimensions of only 0.1 mm per edge. These results suggest that the solubility of tantalum in KOH solutions is much less than that of the niobium analog. To promote higher solubility, the KOH concentration was increased to 30 molar and the reaction temperature increased to over 600 °C.

In these highly concentrated solutions, KT crystals (Fig. 2a) were grown at 640 °C with dimensions of 1.5–2 mm. A single crystal structure was obtained from this reaction and the data is presented in Table 1. These crystals exhibit good optical clarity with only minimal cracking. Only one quality issue is apparent, a slight blue coloration attributed to tantalum reduction can be seen. As in the case of KN, the coloration can be removed by altering the conditions to promote slower growth in order to yield high quality crystals.

3.3. Spontaneous nucleation of $KTa_{1-x}Nb_xO_3$

The ability to control and evenly distribute tantalum and niobium throughout a KTN crystal is a challenge that must be met to ensure good optoelectronic performance. Homogeneity and the ratio of niobium to tantalum are central to accessing KTN's exceptional properties. Slight changes in the ratio can have drastic effects on the Curie temperature, not to mention the potential phase changes at room temperature. A KTN feedstock with the appropriate ratio will ensure the best chance of success, especially considering the homogeneity requirements coupled with the large solubility difference between KT and KN. A KTN feedstock was synthesized by a solid state technique that is detailed in the experimental section 2.2. The final KTN composition was 40% niobium and 60% tantalum, which should optimize the electro-optic effects and have a Curie temperature slightly above room temperature.

The initial KTN growth reaction was performed in a solution of 20 M KOH heated to 575 °C. The resultant crystals consisted primarily of orthorhombic $KNbO_3$. Energy dispersive X-ray (EDX) analysis was able to identify some tantalum content in a small number of crystals. However, the concentration was between 2 and 5 mol%, falling very short of the 60% goal. A general conclusion of low tantalum solubility at this temperature and mineralizer molarity led to the formation of a disproportioned solution skewed heavily towards high niobium concentrations resulting in KN crystallization. To address this, a reaction was performed with conditions of 30 M KOH and 640 °C. However, even at these conditions the KTN feedstock is not congruently saturating. Analysis on the crystals found to contain both metal centers consisted of 20–40% tantalum, indicating tantalum is now solubilizing better at the higher temperature and molarity. Still the main obstacle to forming KTN crystals is suppressing the $KNbO_3$ phase formation. It was speculated that the orthorhombic niobate phase was crystallizing before the solution was congruently saturated with both metal centers.

To slow crystal genesis, the temperature gradient along the ampoule was reduced from 120 to 50 °C. In addition, the temperature in the lower section was raised to 660 °C to further increase tantalum solubility. Under the established gradient, all examined crystals were cubic KTN with an average tantalum concentration of 56%. The quality of these crystals was suitable to get a structure solution with a R-factor of 0.0109. The size of the crystals is promising for future transport growth. The crystals, Fig. 2b, have a slight blue coloration indicating minimal reduction of the metal centers. To eliminate the metal reduction issue the gradient could possibly be tightened even more to promote slower growth. Further steps can be taken by inclusion of an oxidant such as KNO_3, but this would require the use of gold or platinum ampoules.

The measured composition of 56% is acceptable to access KTN's desirable properties. By observing individual spots (Table 2) and elemental mapping using EDX, the homogeneity of a single crystal was explored. In the scanning electron microscope (SEM) picture, Fig. 3, the tantalum to niobium content in the crystal is clearly homogenous. Thus both the ratio and homogeneity difficulties faced by the common melt techniques have been overcome in hydrothermal fluids to produce single crystals of KTN.

3.4. Infrared spectroscopy of KT–KTN–KN

Hydrothermal growth has an inherent risk of incorporating undesired amounts of solvent in crystalline materials. In some cases, simple oxide based materials can be completely transformed into new hydrated or hydroxide species. These concerns in $KNbO_3$ were first explored by Goh and Lange [40]. Infrared studies revealed the inclusion of water and hydroxyl groups in hydrothermal $KNbO_3$ powders synthesized at 200 °C in 6 M KOH. Also utilizing thermogravimetric analysis they were able to determine an approximate composition of $K_{0.95}Nb_{0.99}O_{2.92}(OH)_{0.08} \cdot 0.05H_2O$. While only small amounts of water and hydroxide are present, this can have very detrimental effects on the nonlinear properties. As our studies used extreme concentrations of KOH to crystallize KN, KT, and KTN there was some concern over the possibility of these inclusions. Therefore an infrared spectrum, Fig. 4, for each material was taken from 400 to 4000 cm. The broad peak visible in all three spectra from 600 to 650 cm is attributed to the $v3$ mode of the corner shared NbO_6 and TaO_6 octahedra [42–46]. The areas of interest for water and hydroxide have none of the characteristic peaks in any of the spectra.

Table 2
Energy dispersive X-ray analysis of $KTa_{1-x}Nb_xO_3$.

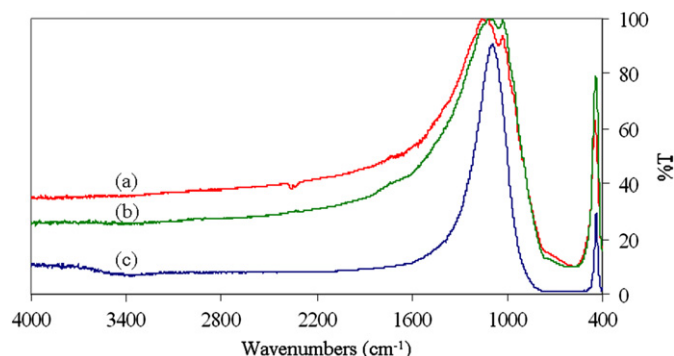| Element	Spot 1	Spot 2	Spot 3	Spot 4
O (at%)	60.50	60.30	60.45	60.91
K (at%)	19.72	19.80	19.65	19.76
Nb (at%)	8.61	8.98	8.65	8.78
Ta (at%)	11.17	10.91	11.25	10.55
$X=$	0.435	0.451	0.434	0.454

Fig. 4. Infrared spectrums from 400 to 4000 cm. (a) KT; (b) KTN; (c) KN.
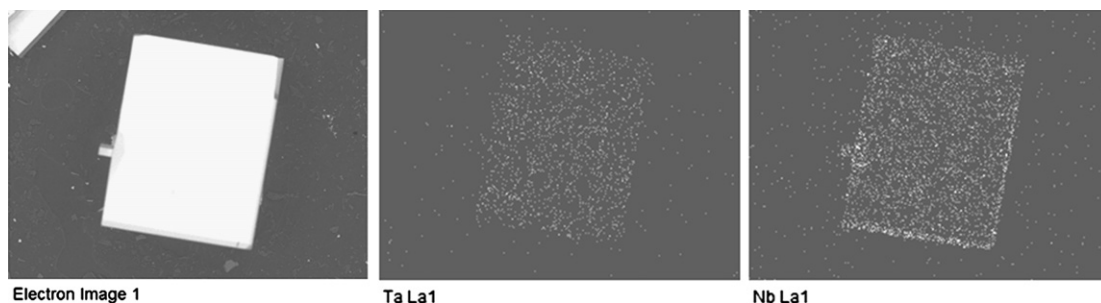

Fig. 3. SEM image of a KTN crystal demonstrating homogeneous distribution of tantalum and niobium.

The lack of hydroxide or water in our crystals grown at much higher temperatures compared to Goh's samples may be explained by studies performed by Shafer and Roy [47,48] on sesquioxide formation in hydrothermal fluids. They reported the formation of YO(OH) or Y(OH)$_3$, at synthesis temperatures below 700 °C. However, at elevated temperatures the two hydroxide species are suppressed in favor of the Y$_2$O$_3$ phase. Their studies also outlined the transition temperatures for a variety of other simple oxide materials. The temperature can vary greatly dependent on the material. While no study has been conducted in regards to the KT–KTN–KN system, the lack of hydroxide present may be attributed to our high synthesis temperatures. It is a general observation that fluids at much higher temperatures and hydroxide concentrations are more "anhydrous" than aqueous fluids at lower temperatures.

4. Conclusions

Successful crystal growth of the each component of the KT–KTN–KN family has been achieved in concentrated KOH supercritical fluids. Somewhat surprisingly, KN crystals of the desired *Amm$_2$* phase formed exclusively even though it grew above the phase transition temperature. The crystals are optically clear with only a slight blue coloration due to reduction of the metal center showing potential for hydrothermal transport growth of larger crystals. Crystals of KTaO$_3$ also demonstrated good optically quality, while providing tantalum growth conditions necessary for KTN synthesis.

Growth of KTa$_{1-x}$Nb$_x$O$_3$ crystals with a composition of $x = 0.44$ were spontaneously nucleated from a 30 M KOH solution and shown by elemental mapping to have a homogenous distribution of tantalum and niobium. Furthermore, infrared analysis has demonstrated that all three members are defect free from any water or hydroxyl inclusions within the crystalline lattice. To date the spontaneous nucleated crystals of all three species are the largest grown by the hydrothermal method.

References

[1] H. Kato, A. Kudo, Chem. Phys. Lett. 295 (1998) 487–492.
[2] Y. Uematsu, Jpn. J. Appl. Phys. 13 (1974) 1362–1363.
[3] B. Li, Y. Hakuta, H. Hayashi, J. Supercrit. Fluid. 35 (2005) 254–259.
[4] P. Gunter, Opt. Commun. 11 (1974) 285–290.
[5] M. Zgonik, K. Nakagawa, P. Gunter, J. Opt. Soc. Am. B. B12 (1995) 1416–1421.
[6] P. Gunter, Jpn. J. Appl. Phys. 16 (1977) 1727–1728.
[7] M. Zgonik, R. Schlesser, I. Biaggo, E. Voit, J. Tscherry, P. Guenter, J. Appl. Phys. 74 (1993) 1287–1297.
[8] P. Gunter, Ferroelectrics 18 (1978) 27–38.
[9] D. Fluck, P. Gunter, Opt. Commun. 147 (1998) 305–308.
[10] D. Guzun, Y. Li, M. Xiao, Opt. Commun. 180 (2000) 367–371.
[11] P. Gunter, Phys. Rep. 93 (1982) 199–299.
[12] K. Yamanouchi, Y. Wagatsuma, H. Odagawa, Y. Cho, J. Eur. Ceram. Soc. 21 (2001) 2791–2795.
[13] B.T. Matthias, J.P. Remeika, Phys. Rev. 82 (1951) 727–729.
[14] V.K. Yanovsky, V.I. Voronkova, J. Cryst. Growth 52 (1981) 654–659.
[15] V.I. Chani, K. Shimamura, T. Fukuda, Cryst. Res. Tech. 34 (1999) 519–525.
[16] J.J. Hurst, A. Linz, Mater. Res. Bull. 6 (1971) 163–168.
[17] W. Xing, H. Looser, H. Wüest, H. Arend, J. Cryst. Growth 78 (1986) 431–437.
[18] J. Hulliger, R. Gutmann, H. Wüest, J. Cryst. Growth 128 (1993) 897–902.
[19] T. Fukuda, Y. Uematsu, Jpn. J. Appl. Phys. 11 (1972) 163–169.
[20] T. Fukuda, Y. Uematsu, T. Ito, J. Cryst. Growth 24/25 (1974) 450–453.
[21] S. Dezhong, Mater. Res. Bull. 21 (1986) 1375–1382.
[22] Y. Kalisky, G. Metrat, N. Muhlstein, A. Brenier, G. Boulon, Opt. Commun. 225 (2003) 377–382.
[23] H. Kimura, K. Maiwa, Z.X. Cheng, C.V. Kannan, Opt. Mater. 30 (2007) 198–200.
[24] K. Nakamura, J. Miyazu, M. Sasaura, K. Fujiura, Appl. Phys. Lett. 89 (2006) 131115–131130.
[25] A.L. Gentile, F.H. Andres, Mater. Res. Bull. 2 (1967) 853–859.
[26] X. Wang, J. Wang, Y. Yu, H. Zhang, R.I. Boughton, J. Cryst. Growth 293 (2006) 398–403.
[27] P.W. Whipps, J. Cryst. Growth 12 (1972) 120–124.
[28] J.Y. Wang, Q.C. Guan, J.Q. Wei, M. Wang, Y.G. Liu, J. Cryst. Growth 116 (1992) 27–36.
[29] M. Sasaura, T. Imai, H. Kohda, S. Tohno, M. Shimokozono, H. Fushimi, K. Fujiura, S. Toyoda, K. Enbutsu, A. Tate, K. Manabe, T. Matsuura, T. Kurihara, J. Cryst. Growth 275 (2005) e2099–e2104.
[30] R. Ilangovan, S. Balakumar, C. Subramanian, P. Ramasamy, Mater. Chem. Phys. 36 (1993) 174–176.
[31] D.J. Marshall, R.A. Laudise, Int. Conf. Cryst. Growth (1966) 557–561.
[32] T. Ishihara, N.S. Baik, N. Ono, H. Nishiguchi, Y. Takita, J. Photochem. Photobio. A 167 (2004) 149–157.
[33] C.K. Tan, G.K.L. Goh, W.L. Cheah, Thin Film Solid 515 (2007) 6577–6581.
[34] J. Bursik, I. Drbohlav, P. Vanek, V. Zelezny, J. Eur. Ceram. Soc. 24 (2004) 455–462.
[35] V. Zelezny, J. Bursik, P. Vanek, J. Eur. Ceram. Soc. 25 (2005) 2155–2159.
[36] I.T. Weber, N. Audebrand, V. Bouquet, M. Guilloux-Viry, A. Perrin, Solid State Sci. 8 (2006) 606–612.
[37] Y. He, Y. Zhu, N. Wu, J. Solid State Chem. 177 (2004) 2985–2990.
[38] J.W. Liu, G. Chen, Z.H. Li, Z.G. Zhang, Int. J. Hydrogen Energy 32 (2007) 2269–2272.
[39] G.M. Sheldrick, SHELXTL, Version 6.1 Structure Determination Software Programs, Bruker Analytical X-ray Systems Inc., Madison, 2001.
[40] G.K.L. Goh, F.F. Lange, J. Mater. Res. 18 (2003) 338–345.
[41] J.F. Liu, X.L. Li, Y.D. Li, J. Cryst. Growth 247 (2003) 419–424.
[42] M. Tatsumisago, A. Hamada, T. Minami, M. Tanaka, J. Non-Cryst. Solid 56 (1983) 423–428.
[43] J.S. de Andrade, A.G. Pinheiro, I.F. Vasconcelos, J.M. Sasaki, J.A.C. de Paiva, M.A. Valente, A.S.B. Sombra, J. Phys. Condens. Matter 11 (1999) 4451–4460.
[44] D. Anderson, K.L. Abdul, S.M. Thomas, M.L. Marcio, M.M. Franklin, M.R. Luiz, Chem. Mater. 20 (2008) 5253–5259.
[45] M.G. Zuev, A.A. Fotiev, M.P. Tsvetkova, J. Mol. Struct. 115 (1984) 79–82.
[46] L.N. Ignat'eva, T.F. Antokhina, S.A. Polishchuk, N.N. Savchenko, E.B. Merkulov, V.M. Buznik, Glass Phys. Chem. 25 (1999) 523–526.
[47] M.W. Shafer, R. Roy, Z. Anorg. Allg. Chem. 276 (1954) 275–288.
[48] M.W. Shafer, R. Roy, J. Am. Ceram. Soc. 42 (1959) 563–580.